

Oxidized phosphatidylserine–CD36 interactions play an essential role in macrophage-dependent phagocytosis of apoptotic cells

Michael E. Greenberg,^{1,3} Mingjiang Sun,¹ Renliang Zhang,^{1,3} Maria Febbraio,¹ Roy Silverstein,¹ and Stanley L. Hazen^{1,2,3}

¹Department of Cell Biology, ²Department of Cardiovascular Medicine, and ³Center for Cardiovascular Diagnostics and Prevention, Cleveland Clinic Foundation, Cleveland, OH 44195

The phagocytosis of apoptotic cells within an organism is a critical terminal physiological process in programmed cell death. Evidence suggests that apoptotic cell engulfment and removal by macrophages is facilitated by phosphatidylserine (PS) displayed at the exofacial surface of the plasma membrane; however, neither the macrophage receptors responsible for PS recognition, nor characterization of the PS molecular species potentially involved, have been clearly defined. We show that the class B scavenger receptor CD36 plays an essential role in macrophage clearance of apoptotic cells *in vivo*. Further, macrophage recognition of apoptotic cells via CD36 is shown to occur via interactions with membrane-associated oxidized PS (oxPS) and, to a lesser extent, oxidized phosphatidylcholine, but not nonoxidized PS molecular species. Mass spectrometry analyses of oxPS species identify structures of candidate ligands for CD36 in apoptotic membranes that may facilitate macrophage recognition. Collectively, these results identify oxPS–CD36 interactions on macrophages as potential participants in a broad range of physiologic processes where macrophage-mediated engulfment of apoptotic cells is involved.

CORRESPONDENCE

Stanley L. Hazen:
hazens@ccf.org

Abbreviations used: CMFDA, 5-chloromethylfluorescein diacetate; Di-I, 1,1'-dioctadecyl-3,3,3',3'-tetramethylindocarbocyanine perchlorate; IRES, internal ribosome entry signal; MPM, mouse peritoneal macrophage; MPO, myeloperoxidase; m/z, mass-to-charge ratio; oxLDL, oxidized low density lipoprotein; oxPC, oxidized PC; oxPC_{CD36}, oxidized PC species possessing an sn-2 acyl group that incorporates a terminal γ -hydroxy(or oxo)- α,β -unsaturated carbonyl; oxPS, oxidized PS; oxPS_{CD36}, oxidized PS species possessing an sn-2 acyl group that incorporates a terminal γ -hydroxy(or oxo)- α,β -unsaturated carbonyl; PAPS, 1-palmitoyl-2-arachidenoil-sn-glycero-3-phosphoserine; PC, phosphatidylcholine; PLPS, 1-palmitoyl-2-lineoyl-sn-glycero-3-phosphoserine; POPC, 1-palmitoyl-2-oleoyl-sn-glycero-3-phosphocholine; POPS, 1-palmitoyl-2-oleoyl-sn-glycero-3-phosphoserine; PS, phosphatidylserine; PSR, PS receptor; SUV, small unilamellar vesicle.

The terminal phase of programmed cell death, removal of apoptotic cells, is a critical homeostatic function involved in an array of diverse cellular processes ranging from embryonic development and tissue remodeling to resolution of inflammation (1, 2). Controlled phagocytic engulfment of apoptotic cells suppresses inflammation by limiting cytolysis and necrosis (2–4). Multiple receptors are implicated in macrophage clearance of apoptotic cells including CD36, a prototypic member of the class B scavenger receptor family (5–11). *In vitro* studies suggest a role for the CD36 scavenger receptor in the recognition of apoptotic cells because both endogenous (e.g., macrophages and dendritic cells) and ectopic (e.g., melanoma cells and fibroblasts) expression of CD36 on the surface of cells confers phagocytic activity for engulfment of apoptotic cells (8, 12, 13). Despite the many demonstrations of CD36 recognition of apoptotic cells using *in vitro* model systems, direct demonstration of CD36 involvement in apoptotic cell clearance *in vivo* is lacking.

CD36 is widely expressed on the surface of multiple cell types including macrophages, adipocytes, platelets, microvascular endothelial cells, and specialized epithelial cells. A heavily glycosylated multiligand receptor belonging to the class B scavenger receptor group, CD36 is reported to mediate uptake of oxidized low density lipoprotein (oxLDL), as well as to play a role in diverse cellular processes including foam cell formation, fatty acid transport, engulfment and removal of senescent cells, suppression of angiogenesis, and cell–matrix interactions (7, 8, 10, 14–17). Multiple distinct binding sites on CD36 are reported to facilitate its broad ligand specificity and functions. CD36 interaction with oxLDL is supported via recognition by the N-terminal region of the receptor (18–20). CD36-dependent uptake of oxLDL has been shown to be critical to cholesterol accumulation and subsequent foam cell formation, activities that likely contribute to the observed involvement of CD36 in mouse models of atherogenesis (21, 22).

Until recently, the precise chemical structures of oxidized species in the LDL particle recognized by CD36 were unknown. Recent studies using a combination of cell binding assays, mass spectrometry, and both analytical and synthetic chemistry successfully isolated and structurally defined a novel oxidized phosphatidylcholine (oxPC) species possessing an sn-2 acyl group that incorporates a terminal γ -hydroxy(or oxo)- α,β -unsaturated carbonyl (oxPC_{CD36}) that serves as high affinity ligands for CD36 via the oxLDL site (23, 24). A conserved structural motif within oxidized choline glycerophospholipids that promotes high affinity CD36 binding was defined; namely, a phospholipid with an oxidatively truncated sn-2 acyl group that incorporates a terminal γ -hydroxy(or oxo)- α,β -unsaturated carbonyl. Only trace levels (a few molecules per particle) of the oxPC_{CD36} were required to support CD36 binding, and the enrichment of these ligands was shown in multiple oxLDL preparations and within atherosclerotic lesions (23, 24).

The mechanisms through which CD36 recognizes apoptotic cells have not been clearly defined. Early studies identified an interaction between CD36 and phosphatidylserine (PS)-containing membranes (8, 9, 25), suggesting that PS externalization during the apoptotic process may serve as a trigger for conferring macrophage phagocytosis via scavenger receptor recognition. Studies using recombinant expression systems in conjunction with competitive synthetic peptides and antibodies have identified a putative PS binding site on the receptor (26) distinct from the oxLDL binding domain that facilitates CD36 interactions with PC-containing membranes or liposomes (18–20).

Detailed investigation of both the receptors involved and the nature of the PS ligands in macrophage–apoptotic cell interactions has remained largely unexplored. Although it is generally assumed that native (nonoxidized) PS is the ligand recognized on apoptotic cells by macrophages, a recent study suggests the potential involvement of oxidized PS (oxPS) as well (27). A role for PS–CD36 interactions in recognition of apoptotic cells has been reported using *in vitro* model systems; however, direct demonstration of a role for CD36 in apoptotic cell clearance *in vivo* is lacking. Because the common structural motif within the oxPC_{CD36} ligands previously identified was localized to the esterified sn-2 fatty acid chain (23, 24), we hypothesized that other phospholipid analogues, such as those from oxPS (i.e., an oxPS species possessing an sn-2 acyl group that incorporates a terminal γ -hydroxy(or oxo)- α,β -unsaturated carbonyl [oxPS_{CD36}]), may be able to function as high affinity ligands for CD36, facilitating recognition between the apoptotic cell membrane and CD36 on the macrophage cell surface. This seemed especially plausible because previous reports of CD36-mediated phagocytosis of apoptotic cells via PS failed to consider that oxidation of lipids may be important, and hence, no measures to prevent lipid oxidation were used (8, 9, 25, 26). In this paper, using CD36 KO mice and a wound healing model, we show a direct role for CD36 in apoptotic cell clearance. Moreover, using a combination of both direct binding and competition studies, along with mass spectrometry characterizations, we

now show that oxPS species, but not nonoxidized PS, serve as preferred ligands within apoptotic cells for CD36-mediated phagocytosis by macrophages.

RESULTS

Apoptotic cells accumulate in CD36 KO mice wounds relative to CD36 WT

In full thickness 6-mm punch biopsy wound healing experiments conducted on CD36 KO and WT mice, we noted a two- to threefold increase in apoptotic cell numbers in wounds from CD36 KO mice at multiple time points, consistent with delayed clearance of apoptotic cells in the CD36 mice (Fig. 1). *In vitro* control studies using primary CD36-expressing macrophages isolated from background-matched WT and CD36 KO mice demonstrated no differences in apoptosis rates to apoptogenic triggers such as serum deprivation, staurosporin, or Fas ligand (unpublished data). In addition, both morphometric and histological analyses revealed no observable differences in either the overall rate of wound closure or leukocyte (monocyte and neutrophil) recruitment between CD36 KO and WT animals over a 9-d period after wound injury (unpublished data). Collectively, these results demonstrate that CD36 KO mice have impaired ability to efficiently clear apoptotic cells from an inflammatory setting.

CD36-specific binding and uptake of PS-containing vesicles is mediated by oxidized, not nonoxidized, PS species, as monitored by quantitative flow cytometry

The nature of the ligands on apoptotic cell membranes recognized by macrophage CD36 has not been clearly defined. Although previous data suggest a role for PS, recent experimental studies with CD36–oxLDL interactions showed a requirement for oxidized choline glycerophospholipids. We therefore hypothesized that oxPS, and not PS, might play a role in macrophage CD36 recognition of apoptotic membranes.

Before investigating the ability of CD36 to specifically bind to oxPS, we sought to develop a tractable system with which we could simultaneously monitor CD36 expression, manipulate vesicle, liposome, or lipoprotein lipid composition, and also quantify particle binding. A bicistronic CD36,GFP reporter plasmid containing an internal ribosome entry signal (IRES) was constructed for simultaneous expression of full-length WT human CD36 and GFP. Use of this construct results in GFP expression in constant molar ratio with intact native human CD36 within transfected cells, permitting cellular mean GFP fluorescence to be used as a quantitative measure proportional to CD36 expression. As illustrated in Fig. 2 a, flow cytometry analyses of transiently transfected leukemia (K562) cells with the bicistronic construct resulted in CD36 surface expression at levels that increase proportionately with increasing cellular GFP fluorescence. Similar results were seen using alternative cell types (Jurkat T cells, COS-7 fibroblasts, human embryonic kidney cells, or THP-1 human monocyte/macrophage like

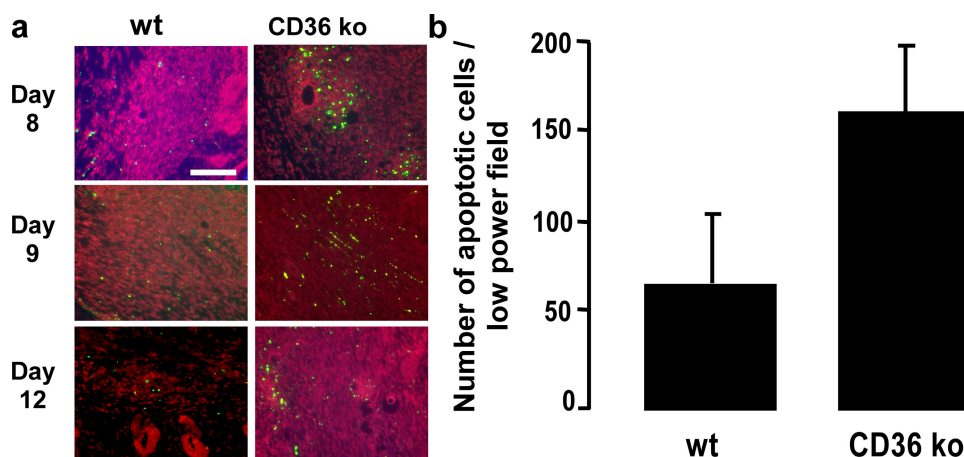


Figure 1. Increased apoptotic cell accumulation in CD36 KO mice wounds compared with WT. (a) Punch biopsy wounds from WT and CD36 KO mice were excised on days 8, 9, and 12 and stained (green) for apoptotic cells using a fluorescein DNA fragmentation kit (see Materials

and methods). Skin is autofluorescent (red). Bar, 500 μm (b) Quantitation of apoptotic cell numbers from WT and CD36 KO wounds (day 8 after wound). Results represent the mean \pm SD for six independent animals per group.

line; unpublished data). Confirmation that the recombinant human CD36 was localized to the cell surface in these systems was achieved by fluorescent microscopy studies using anti-CD36 antibody on fixed, nonpermeabilized cells. Demonstration that surface CD36 was functional in the transfected cells was achieved by showing that cells only bound appreciable levels of 1,1'-dioctadecyl-3,3,3',3'-tetramethylindocarbocyanine perchlorate (Di-I)-labeled oxLDL in the presence of CD36 (Fig. 2 b). Two-color flow cytometry analyses with the described system (GFP fluorescence monitored for measure proportional to cell CD36 expression and Di-I fluorophore for labeled lipoproteins or liposomes) permitted simultaneous monitoring of CD36-specific increases in particle binding across a range of CD36 surface expression levels. This is illustrated in Fig. 2 c, where K562 cells were transiently transfected with either GFP alone (control) or the CD36,GFP bicistronic construct, incubated with Di-I-labeled oxLDL, and analyzed by two-color flow cytometry. A dramatic increase in specific binding of oxLDL in proportion with increasing CD36 expression is noted (Fig. 2, d and e).

We next examined the CD36 binding activity of various molecular species of PS versus oxPS using a fluorescent vesicle system in which presentation of the various PS species was maintained relatively uniform by incorporation of only a minor mole percent of PS within a lamellar phase-preferring carrier lipid, 1-palmitoyl-2-oleoyl-*sn*-glycero-3-phosphocholine (POPC), under the experimental conditions (i.e., temperature) used. Small unilamellar vesicle (SUV) POPC with 1 mol% Di-I and 20 mol% 1-palmitoyl-2-oleoyl-*sn*-glycero-3-phosphoserine (POPS), 1-palmitoyl-2-lineoyl-*sn*-glycero-3-phosphoserine (PLPS), or 1-palmitoyl-2-arachidonyl-*sn*-glycero-3-phosphoserine (PAPS; either as native form or after oxidation by the myeloperoxidase [MPO]- H_2O_2 - NO_2^- system) were generated by extrusion and incubated with CD36-expressing (CD36,GFP bicistronic) versus control-expressing

(GFP only) cells. Remarkably, only oxPS-containing vesicles demonstrated enhanced CD36-specific binding, with the extent of binding proportional to cellular expression of CD36 (Fig. 3). PS species possessing the oxidation-susceptible *sn*-2 linoleic or arachidonic acids were readily converted into CD36 binding ligands by oxidation, whereas PS possessing the relatively nonoxidizable *sn*-2 fatty acid oleic acid did not promote CD36 binding despite exposure to oxidation systems (Fig. 3). These results are consistent with mass spectrometry studies that demonstrated no significant modification of the parent lipid (POPS; unpublished data) but significant formation of multiple oxPS species (Table I) from PLPS- and PAPS-containing vesicles after oxidant exposure.

Macrophages use CD36 to recognize bilayers containing oxidized PS rather than nonoxidized PS species

By using the flow cytometry-based assay developed to monitor vesicle binding, we conclude that oxPS, as opposed to PS, in a membrane bilayer serves as a preferred ligand for CD36 across multiple orders of magnitude of CD36 surface expression on the target transfected cell. Because recombinant systems that expressed CD36 have the potential to inaccurately reflect endogenous CD36-oxPS binding interactions, we performed additional studies to determine whether our observations in transfected cos-7 and K562 cells were representative of endogenous CD36 binding behavior within macrophages. Mouse peritoneal macrophages (MPMs) from WT versus CD36 KO mice were incubated with Di-I-labeled SUVs containing low mole percent PS versus oxPS species, and both immunolocalization of macrophage CD36 and vesicle binding were concomitantly monitored. Marked increases in oxPS binding to WT versus CD36 KO peritoneal macrophages were noted (Fig. 4, a and b), consistent with CD36 serving as the predominant oxPS receptor expressed in mouse macrophages. oxPS binding occurred exclusively in

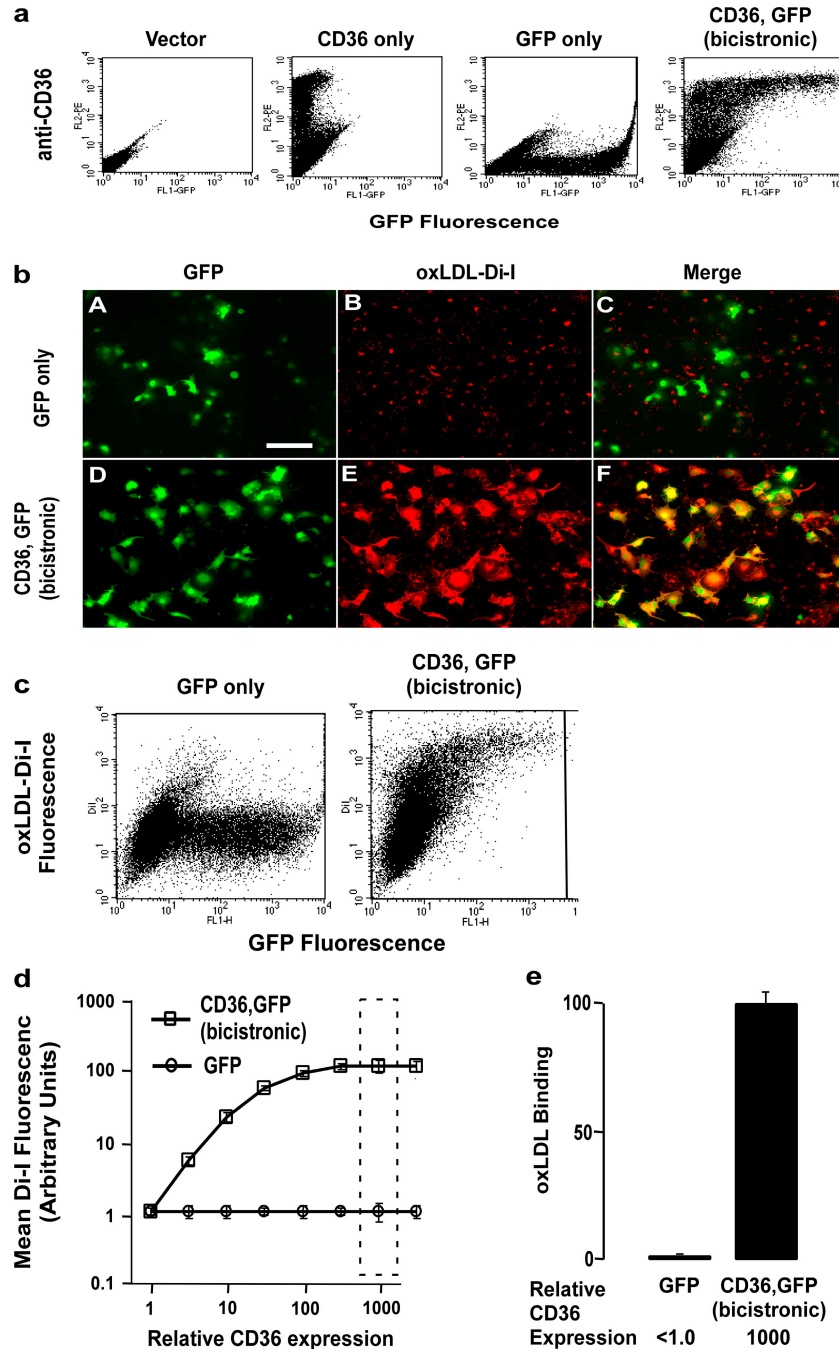


Figure 2. Development of two-color flow cytometry-based binding assay permitting concomitant quantification of CD36 surface expression level and ligand binding. (a) K562 (chronic myelogenous leukemia) cells were transfected with plasmids encoding empty vector (control), only human CD36, only GFP, or both CD36 and GFP using the bicistronic (IRES) vector as described in Materials and methods. Cells were cultured overnight, and cell surface CD36 (CD36-mAb conjugated to phycoerythrin) and GFP fluorescence were simultaneously analyzed by two-color flow cytometry. Note that the bicistronic plasmid expresses cell surface CD36 receptor in a dose-dependent manner as a function of GFP fluorescence. (b) Cos-7 cells were transfected with DNA plasmids encoding either GFP only or both CD36 and GFP proteins using the bicistronic vector. Cells were then incubated at 4°C in the absence versus presence of

oxLDL labeled with the lipophilic dye Di-I), washed, and visualized, as described in Materials and methods. Note that a high degree of Di-I fluorescence (oxLDL binding) is only observed in cells transfected with CD36 and that the cells demonstrating Di-I fluorescence (oxLDL binding) have cellular staining patterns similar to those observed for GFP within the CD36 + GFP bicistronic transfected cells (images D, E, and F). For comparison, only background Di-I fluorescence is seen in cells transfected with GFP only (images A, B, and C). Bar, 50 μm (c) K562 cells transfected with plasmids expressing CD36, GFP (bicistronic) or GFP alone were cultured overnight and incubated with 40 μg/ml oxidized (via the MPO-NO₂⁻-H₂O₂ system) LDL labeled with the lipophilic dye Di-I at 4°C for 30–60 min. After extensive washing to remove unbound oxLDL, CD36 expression (a function of GFP fluorescence) and oxLDL binding (red

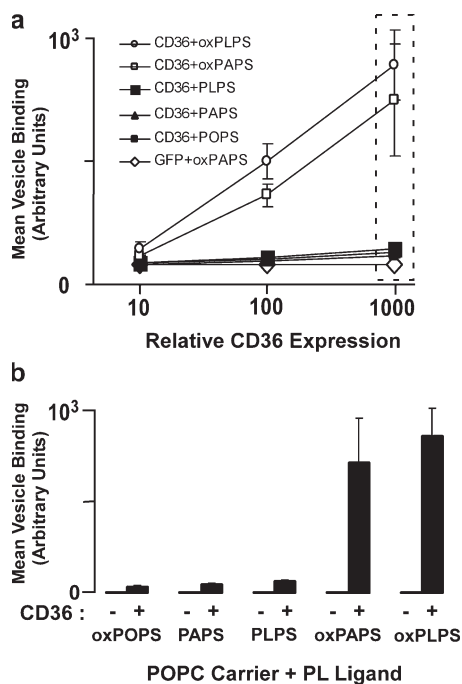


Figure 3. Recombinant CD36 preferentially binds to oxPS-containing lipid vesicles compared with nonoxidized PS-containing vesicles. (a) K562 cells were transfected with plasmids expressing GFP alone (control) or CD36,GFP (bicistronic), cultured overnight, and incubated at 4°C for 1 h with phospholipid vesicles (prepared by extrusion of 80 mol% POPC + 20 mol% of PS [PLPS or PAPS and the lipophilic dye Di-I at 1 mol%]). Before incubation, vesicles were either oxidized (via the MPO-NO₂⁻-H₂O₂ system) or untreated. After extensive washing to remove unbound lipid vesicles, CD36 expression (proportional to GFP fluorescence) and the corresponding amount of fluorescent lipid ligand bound (Di-I fluorescence) were analyzed simultaneously by two-color flow cytometry as in Fig. 2. Panel a shows the mean fluorescence values for triplicate experiments. Open symbols represent oxidized PS liposomes, closed symbols represent untreated (nonoxidized) PS liposomes. (b) Fluorescent liposome binding shown as a function of the single GFP fluorescence intensity interval indicated by the dashed-line rectangle in panel a. Data are expressed as the mean ± SD of triplicate samples and are representative of at least three separate experiments.

WT and not CD36 KO macrophages. Both WT and CD36 KO macrophages also demonstrated low but detectable levels of binding to nonoxidized PS (Fig. 5 b).

Vesicles possessing oxidized PS, but not nonoxidized PS, inhibit phagocytosis of apoptotic cells in a CD36-dependent manner

To explore the potential role of CD36–oxPS interactions in macrophage engulfment of apoptotic cells, we examined the

capacity of SUVs possessing PS versus oxPS species to interfere with macrophage phagocytosis of apoptotic cells. Confluent monolayers of both WT and CD36 KO MPMs were overlaid with viable versus apoptotic HL60 cells. After incubation, nonadherent/nonphagocytosed cells were removed by vigorous washing, and engulfment of apoptotic cells was quantified by in situ peroxidase staining. Fig. 5 a illustrates the assay, with visualization of WT MPMs phagocytosing control (1) or apoptotic (2) peroxidase-containing HL60 cells.

To further explore the role of oxPS in macrophage engulfment of apoptotic cells via CD36, parallel studies were performed in the presence of small unilamellar POPC vesicles containing either low mole percent incorporation of either PS or oxPS as potential competitors of apoptotic cell phagocytosis. As noted in Fig. 5 b, SUVs possessing oxPS were significantly more efficient than those with PS at inhibiting apoptotic cell phagocytosis by WT macrophages. No competitive inhibitory effect of oxPS-containing vesicles was noted in CD36 KO macrophages. CD36 KO macrophages demonstrated enhanced inhibition in apoptotic cell phagocytosis with vesicles containing nonoxidized PS species, consistent with possible adaptive up-regulation of an alternative receptor in the CD36-null mice that recognizes native PS but not oxPS forms.

Because macrophages have multiple potential alternative receptors that could participate in apoptotic cell recognition in vivo (one or more of which appear to be up-regulated in the CD36 KO MPMs), we sought to perform parallel studies examining the involvement of CD36–oxPS interactions in a cell type with low endogenous background levels of PS and oxPS recognition. For these studies we selected COS-7 fibroblasts because transfection of these cells with human CD36 has previously been shown to confer professional phagocytic function to this otherwise nonphagocytic cell (12), and binding studies with the native cells demonstrate low background levels with SUVs containing either PS or oxPS species. In the absence of a competitor, COS-7 cells transfected with human CD36 (but not vector control) demonstrated enhanced phagocytic capacity toward multiple different apoptotic cells (e.g., data for apoptotic HL60 human monocyte/macrophage cells and fluorescently labeled apoptotic Jurkat T cells are shown in Fig. 5 (c and d, respectively)). Co-incubation of vesicles containing oxPS species, but not nonoxidized PS, with apoptotic cells markedly inhibited phagocytosis by the CD36-transfected Cos-7 cells.

Vesicles possessing oxPS more efficiently inhibit macrophage-mediated phagocytosis of apoptotic cells than vesicles containing oxPC

Because both the previously identified family of oxPC_{CD36} ligands and the putative oxPS_{CD36} ligands may share common

fluorescence) were analyzed simultaneously by two-color flow cytometry. A representative flow cytometry dot plot is shown. Note that oxLDL binds to CD36-expressing cells in a dose-dependent fashion (i.e., with increasing CD36 expression there is a corresponding increase in oxLDL binding). (d) The mean oxLDL-Di-I fluorescence is plotted against the relative CD36

expression levels as monitored by the mean GFP fluorescence intensity from triplicate binding experiments shown in panel a. (e) LDL binding is shown for the single CD36 expression level (as measured by the GFP fluorescence intensity interval), indicated by the dashed-line rectangle in d. Results represent the mean ± SD for three independent experiments.

Table I. Parent ($[M-H]^-$) and characteristic daughter ions (MS2 and MS3) of candidate CD36 ligands from oxidized PAPS and PLPS

PL-PS oxidation products				
m/z	MS2	MS3	Structure of sn-2 side chain	Abbreviations
650.3	563.3	409/391/307/255/171/153	9-oxononanoic acid	ON-PS
666.3	579.3	409/391/323/255/187/153	Azeleic acid	A-PS
704.3	617.3	409/391/361/255/225/153	9,12-dioxododec-10-enoic acid	KODA-PS
706.3	619.3	409/391/363/255/227/153	9-hydroxy-12-oxododec-10-enoic acid	HODA-PS
720.3	633.3	409/391/377/255/241/153	9-oxo-11-carboxyundec-6-enoic acid	KDdiA-PS
722.3	635.3	409/391/379/255/243/153	9-hydroxy-11-carboxyundec-6-enoic acid	HDdiA-PS
758.3	671.3		Linoleic acid	PL-PS
PA-PS oxidation products				
m/z	MS2	MS3	Structure of sn-2 side chain	Abbreviations
594.3	507.3	409/391/255/251/153/115	5-oxovaleric acid	OV-PS
610.3	523.3	409/391/267/255/153/131	Glutaric acid	G-PS
648.3	561.3	409/391/305/255/169/153	5,8-dioxooct-6-enoic acid	KOOA-PS
650.3	563.3	409/391/307/255/153	5-hydroxy-8-oxooct-6-enoic acid	HOOA-PS
664.3	577.3	409/391/321/255/184/153	5-oxo-7-carboxyhept-6-enoic acid	KOdiA-PS
666.3	579.3	409/391/323/255/187/153	5-hydroxy-7-carboxyhept-6-enoic acid	HOdiA-PS
782.3	695.3		Arachidonic acid	PA-PS

PAPS and PLPS were individually oxidized and analyzed by HPLC with on-line electrospray ionization mass spectrometry on an iontrap instrument using MSⁿ mode. Parent and characteristic MS2 and MS3 daughter ions (for sn-2 ox fatty acid) are shown. Ions in the MS2 spectrum that are produced after neutral loss ($m/z = 87$) of aziridine-2-carboxylic acid (Fig. 8) from the precursor parent ions were optimized and used as the precursor for MS3 experiments. The MS3 ions of the corresponding sn-2 oxidized fatty acids previously identified as CD36 ligands within oxPC species (references 23, 24) were isolated and fragmented. The structure and observed ions of the sn-2 chain of oxPS are shown. These corresponded to the previously identified sn-2 side chains on oxPC that serve as CD36 ligands.

recognition epitopes in the truncated, oxidized sn-2 fatty acid chain, we were interested to test whether oxPC liposomes could compete with oxPS liposomes for binding to CD36-expressing cells. Using the fluorescent binding assay of Di-I-labeled oxPS vesicles incubated with CD36-transfected K562 cells, we added a 10-fold excess (bulk lipid concentration) of unlabeled oxPS- or oxPC-containing SUVs (same mole percent incorporation of oxPS vs. oxPC) to compete for CD36-specific binding. As shown in Fig. 6 a, although excess nonlabeled oxPS SUVs markedly attenuated Di-I-oxPS SUV binding to CD36-expressing cells, a comparable molar excess of oxPC-possessing SUVs had only a modest inhibitory effect. At a single surface expression level of CD36 (Fig. 6 b), note that Di-I-labeled oxPS SUVs demonstrate only modest (~20%) reductions in CD36-specific binding in the presence of a 10-fold excess of oxPC SUVs but at least 90% reduction in binding in the presence of comparable incubations with excess unlabeled oxPS SUVs.

To further examine the relative contribution of oxPS versus oxPC in macrophage recognition of apoptotic cells, MPMs from WT mice were incubated with apoptotic cells in the absence versus presence of similar SUV preparations comprised of POPC only or POPC carrier plus 20 mol% of the indicated nonoxidized versus oxPC and oxPS molecular species (Fig. 6 c). Most notable was that all SUVs comprised of only nonoxidized phospholipids failed to inhibit MPM phagocytosis of apoptotic cells. Further, although addition of oxidized 1-palmitoyl-2-arachidenoyle-3-glycero-3-phosphocholine-containing vesicles (but not 1-palmitoyl-2-

arachidenoyle-3-glycero-3-phosphocholine) partially inhibited macrophage phagocytosis of apoptotic cells, the effect was only modest. In contrast, SUVs containing oxPS but not nonoxidized PS molecular species (1,2-dipalmitoyl-sn-glycero-3-phosphoserine, POPS, or PLPS) markedly inhibited macrophage engulfment of apoptotic cells. Collectively, these data support a major role for macrophage-mediated phagocytosis of apoptotic cells via CD36 interaction with apoptotic membrane oxPS species. They also suggest that oxPC species can participate, albeit to a lesser degree, in apoptotic cell recognition via CD36.

Enrichment of oxidized PS species, but not nonoxidized PS, within cellular membranes of nonapoptotic cells promotes enhanced CD36-dependent phagocytosis by macrophages

To independently confirm that enrichment of oxPS within membranes confers CD36-dependent recognition, we performed a series of studies where oxPS versus PS was integrated into the plasma membranes of viable cells, and their phagocytosis by WT versus CD36 KO macrophages was quantified. For these studies, enrichment of plasma membrane lipids was achieved as described in Materials and methods, with incorporation of either POPC carrier alone or with addition of low mole percent (16 mol%) incorporation of either PAPS or oxidized PAPS species. Both the oxPS- and PS-enriched HL60 cells showed similar enhancement in annexin V staining compared with control (POPC carrier lipid) treated cells, suggesting similar levels of phosphatidylserine exposure (nonoxidized and oxidized) at the plasma membrane (Fig. 7 a). Enriching the

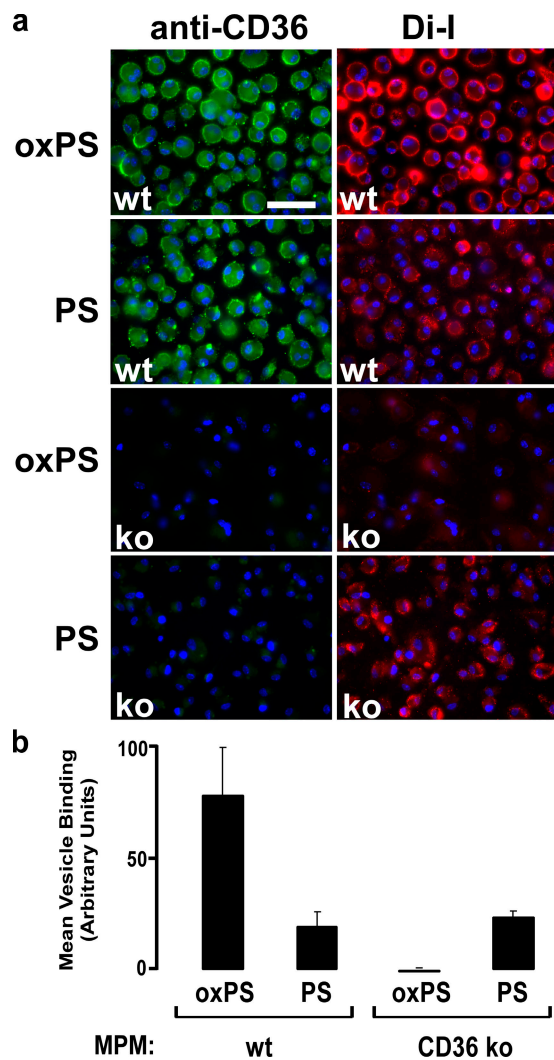


Figure 4. oxPS ligands show higher affinity for CD36 in vivo than PS. (a) Thioglycollate-elicited MPMs from CD36 WT and CD36 KO mice were incubated with Di-I-labeled oxPS- or PS-containing POPC vesicles prepared as in Fig. 3. The extent of direct vesicle binding was visualized by fluorescent microscopy of the Di-I fluorophore and counterstained with anti-mouse CD36 antibody followed by goat anti-mouse IgA secondary antibody conjugated to fluorescein isothiocyanate (shown in anti-CD36 column). Bar, 50 μm (b) The relative amounts of lipid binding were determined by quantifying the surface Di-I fluorescence from the micrograph in Fig. 4 a using ImagePro software. Results represent the mean \pm SD of three independent experiments.

plasma membranes of viable (nonapoptotic) HL60 cells with oxPS markedly increased their phagocytosis by WT (CD36-expressing) MPMs, whereas no increase was noted with nonoxidized PS (Fig. 7 b). Interestingly, in contrast to WT macrophages, plasma membrane integration of nonoxidized PS resulted in more efficient binding and phagocytosis by CD36 KO MPMs (Fig. 7 c), again suggesting an apparent adaptive up-regulation of an alternative receptor for PS (nonoxidized forms only) in the CD36-null MPMs.

Mass spectrometry analysis of oxPS species suggests possible candidate ligands for CD36 in apoptotic cell membranes in vivo

Previously, we determined that a novel family of oxPC species with enhanced CD36 binding activity formed in vivo (i.e., oxPC carrying an oxidatively truncated sn-2 acyl group with a terminal γ -hydroxy(or oxo)- α,β -unsaturated carbonyl) (23, 24). We were therefore interested to determine whether structural analogues of these CD36 ligands containing a PS headgroup are formed during apoptosis and PS oxidation and might thus mediate CD36-dependent recognition of apoptotic cell membranes. We performed extensive characterization of PAPS- and PLPS-derived oxidation products from synthetic precursor lipids (PAPS and PLPS) and apoptotic cell membranes using multiple mass spectrometric approaches (including MSⁿ) to determine if the anticipated oxPS analogues were formed.

Initially, oxPS species were generated and characterized by taking SUVs comprised of relatively oxidant-resistant carrier lamellar phase phospholipid (POPC) and trace levels (10–20 mol%) of either PAPS or PLPS and exposing them to a physiological oxidation system (MPO–H₂O₂–NO₂[−] system) as described in Materials and methods. The resultant lipids were fractionated by reverse phase HPLC and examined on-line by electrospray ionization mass spectrometry (MSⁿ mode) using an ion-trap instrument. A previous study (28) showed that PS species undergo characteristic fragmentation patterns under negative ion electrospray ionization conditions (Fig. 8). Our analyses confirmed this. We used this information to initially identify candidate oxPS species by monitoring for ions that demonstrated neutral loss of aziridine-2-carboxylic acid daughter (MS₂) ions with characteristic loss of 87 amu (Fig. 8 and Table I). Comparisons with the calculated theoretical mass of expected oxPS species generated reveal that besides the oxygenated long chain species, products with oxidatively truncated sn-2 fatty acids were also observed in the spectra. Among them, the molecular ions of sn-2 oxidized fatty acids from CD36 oxPC analogue ligands were also present (Table I). To confirm this, ions in MS₂ spectra that are produced after neutral loss of aziridine-2-carboxylic acid from the precursor ions (parent oxPS) were collisionally dissociated, and MS₃ ions were identified. Both individual corresponding synthetic oxPC_{CD36} (23, 24), as well as theoretical ions and the fragmentation pattern of sn-2 chains of the CD36 ligands, were calculated in parallel and compared with the ions directly monitored in oxPS MS₃ spectra (Table I). The observation of the expected ions of sn-2 side chains in the MS₃ spectrum provides additional evidence for the presence of the indicated specific oxPS (Table I), the structural analogues of previously reported oxPC_{CD36} ligands (23, 24). From this we conclude that oxPS_{CD36} lipid ligands, structural and chemical analogues of oxPC_{CD36}, were generated upon oxidation of PAPS and PLPS and may thus potentially serve as recognition ligands for CD36-mediated phagocytosis of apoptotic cells.

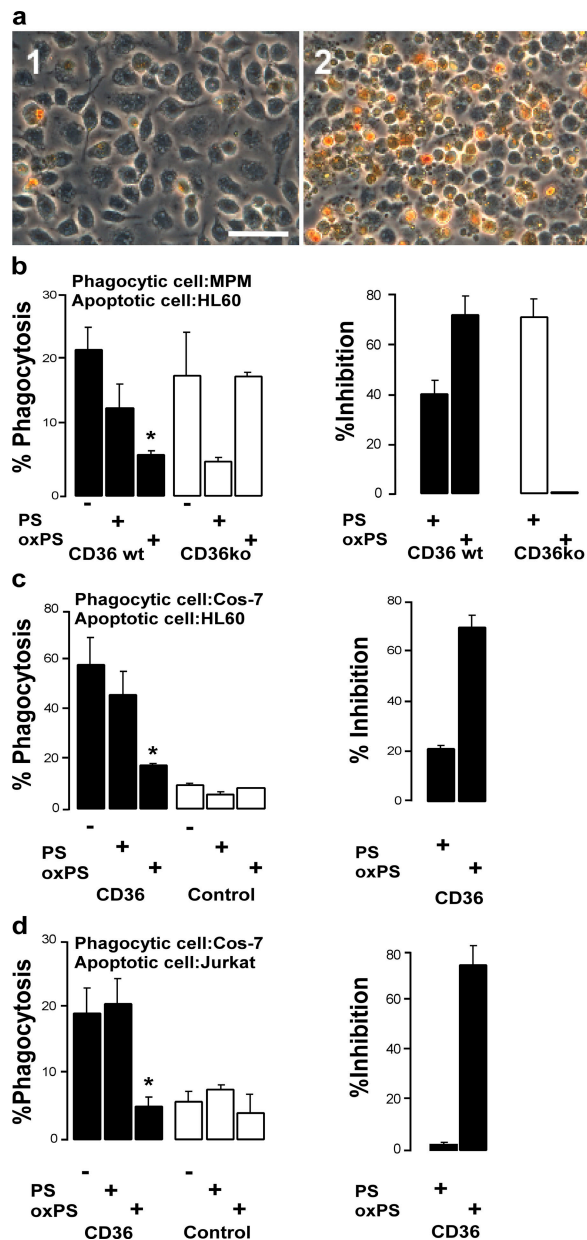


Figure 5. Co-incubation with oxPS vesicles competitively inhibits CD36-dependent phagocytosis of apoptotic cells. Phagocytosis assay of (a, 1) 10^6 untreated and (a, 2) 10^6 UV-irradiated apoptotic (as monitored by DNA laddering assay and annexin V staining) HL60 cells overlaid onto 10^5 CD36 WT MPMs and incubated for 1 h at 37°C , followed by extensive washing with PBS to remove noningested and unbound apoptotic cells. Cells were stained with dimethylbenzidine (o-dianisidine), as described in Materials and methods, to reveal bound and phagocytosed HL60 cells that appear brownish-yellow in color. Bar, $50\ \mu\text{m}$ (b) UV-irradiated HL60 cells were combined with lipid vesicles and overlaid onto CD36 WT or KO MPMs and incubated for 1 h at 37°C . After extensive washing, bound and ingested HL60 cells were revealed by in situ peroxidase (dimethylbenzidine) staining. (left) Total number of macrophage-associated (bound or ingested) HL60 cells in the presence of POPC vesicles containing 20 mol% PS or oxPS compared with no lipid vesicle co-incubation. (right) Percent inhibition of apoptotic HL60 cell association with MPMs conferred by oxPS- versus 20 mol% PS-containing POPC liposomes, as

To confirm formation of oxPS species in apoptotic cell membranes, such as those possessing an oxidatively truncated sn-2 acyl group with a terminal γ -hydroxy(or oxo)- α,β -unsaturated carbonyl, a series of experiments were performed with membrane extracts. Recovered lipids were analyzed by LC/ESI/MS/MS analyses, and specific oxPS species were identified by their characteristic retention times and mass-to-charge ratio (m/z) of parent/daughter ion transitions using multiple reaction monitoring mode, as described in Materials and methods. In separate parallel analyses, the structure of the sn-2 oxidized fatty acid on the indicated oxPS species was further confirmed using MS^n mode. Multiple specific oxPS species possessing mass spectral characteristics indicative of oxPS harboring oxidatively truncated sn-2 fatty acids (Fig. 9) analogous to oxPC species previously shown to serve as CD36 ligands were identified, suggesting that these structurally defined oxPS species may serve as potential CD36 ligands on apoptotic cells.

DISCUSSION

This paper demonstrates a key role for CD36 in recognition of apoptotic cells in vivo. Further, macrophage recognition of apoptotic cells via the scavenger receptor CD36 is shown to occur virtually exclusively through interactions with oxPS, and to a lesser extent oxPC, but not nonoxidized PS, molecular species. The mass spectrometry studies performed also demonstrate the presence of potential candidate structures of specific oxidized PS species within apoptotic cell membranes that may serve as ligands for the scavenger receptor CD36, based on their structural homology to recently defined oxPC molecular species possessing a high affinity recognition motif for CD36 interaction (23, 24). Current dogma proposes that the initial triggering event for macrophage phagocytic recognition of apoptotic cells is the flipping of PS to the exofacial surface, enabling scavenger receptors to engage and facilitate macrophage engulfment of the apoptotic cell. The present results suggest that an oxidative event may also be a prerequisite to macrophage phagocytosis of apoptotic cells via scavenger receptor CD36–PS interactions. Whether such an oxidative event occurs within apoptotic cell membrane lipids before or after PS flips to the exofacial surface after exposure to an apoptogenic stimulus remains unknown. Further, given the multiple

determined by $([\text{number of untreated control cells} - \text{number of PS or oxPS-co-incubated cells}] / \text{number of untreated control cells}) \times 100$. Note that POPC vesicles containing oxPS competitively inhibit the binding of apoptotic HL60 cells to CD36 WT MPMs compared with CD36 KO MPMs. (c) A similar experiment to that in b, with apoptotic HL60 cells overlaid onto CD36- or vector-transfected (control) Cos-7 cells (used as the phagocytic cell) and incubated with POPC vesicles containing either 20 mol% PS or oxPS. (d) A similar experiment conducted with UV-irradiated apoptotic Jurkat T cells fluorescently labeled with CellTracker Green CMFDA as a marker for phagocytized cells, overlaid onto CD36- or vector-transfected (control) Cos-7 cells and co-incubated with the indicated PS- versus oxPS-containing vesicle. *, $P < 0.02$ versus control.

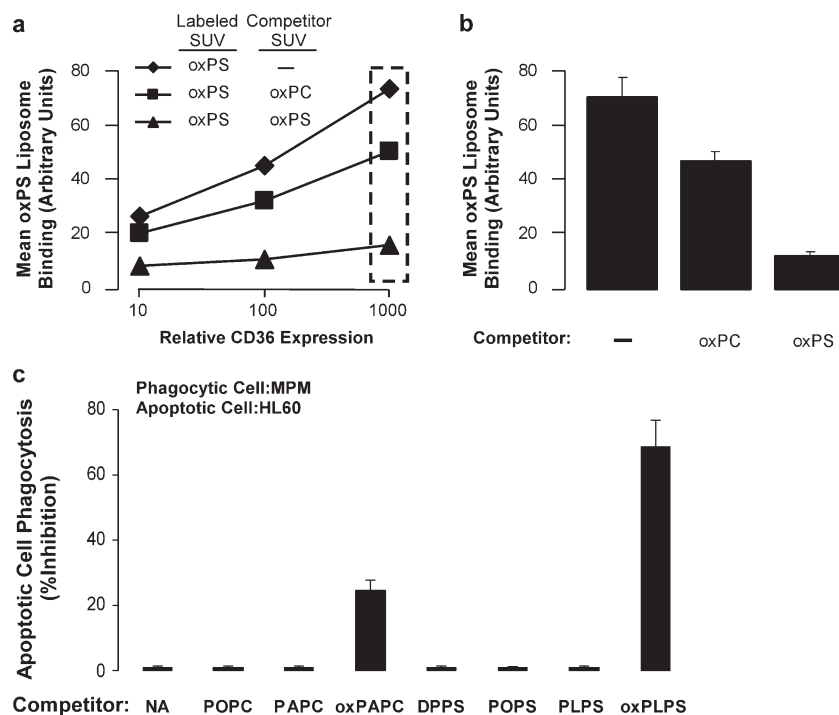


Figure 6. Co-incubation with oxPS versus oxPC vesicles reveals a primary role for oxPS-CD36 interactions in macrophage phagocytosis of apoptotic cells. (a) K562 cells transfected with plasmids expressing CD36,GFP (bicistronic) were cultured overnight and incubated with POPC vesicles containing 20 mol% oxidized PAPS (oxPS) labeled with the lipophilic dye Di-I at 4°C for 30–60 min in the presence or absence of a 10-fold excess of either unlabeled oxPLPC (oxPC) or oxPS vesicles (20 mol% in POPC). After extensive washing to remove unbound vesicles, CD36 expression and oxPS binding (red fluorescence) were analyzed

simultaneously by two-color flow cytometry. (b) oxPS vesicle binding is shown for the single CD36 expression level indicated by the dashed-line rectangle in panel a. Results represent the mean \pm SD for three independent experiments. (c) 10^6 UV-irradiated apoptotic HL60 cells were overlaid onto 10^5 CD36-expressing (WT) MPMs and incubated for 1 h at 37°C, in the presence or absence of the indicated lipid-containing vesicles (made in POPC at 20 mol%). After extensive washing, bound and ingested HL60 cells were revealed by in situ peroxidase (dimethylbenzidine) staining.

alternative receptors involved in apoptotic cell clearance and their varied expression levels within different tissues and conditions, the relative contribution of oxPS-CD36 interactions to apoptotic cell clearance mechanisms in vivo is not clear. It seems reasonable to speculate that CD36-oxPS interactions may play a more prominent role at sites where lipid peroxidation is enhanced, such as during inflammation.

A critical role for oxPS species in apoptotic cell recognition by macrophage CD36 is supported by multiple independent lines of evidence. We monitored oxPS liposome binding as a function of cell surface CD36 levels using a novel fluorescence-based assay and observed that liposomes containing oxPS, but not nonoxidized PS, preferentially bind to CD36-transfected cells. Complementary studies using WT and CD36 KO MPMs confirm a requirement for oxidation of PS for cell binding and phagocytosis via endogenously expressed CD36 in macrophages. Further, incorporation of oxPS, but not PS, into viable nonapoptotic cell membranes was shown to confer CD36 binding activity and the capacity to be phagocytosed by CD36-bearing cells. Studies using multiple distinct cells and apoptotic triggers confirm a critical role for oxPS versus PS as recognition ligands for CD36-mediated phagocytosis. Finally, using multiple mass spectrometry-based

approaches, we show that oxPS species possessing a structurally conserved CD36 recognition motif—an sn-2 acyl group that incorporates a terminal γ -hydroxy(or oxo)- α,β -unsaturated carbonyl—are formed within apoptotic membranes and may thus play a role in CD36-dependent recognition of apoptotic cells.

The multiligand receptor CD36 is one of several receptors implicated in mediating phagocyte recognition of apoptotic cells during engulfment. Other receptors potentially involved in apoptotic cell clearance include SRB1, SRA, LOX-1, CD68, CD14, and the recently cloned protein with reported binding activity for PS-containing membranes, the PS receptor (PSR) (11). Numerous lines of evidence have supported a role for receptor-mediated recognition of PS on the surface of apoptotic cells. It is interesting to note that all of these receptors, aside from PSR, were originally described to bind oxLDL. Indeed, CD36 and other scavenger receptors are thought to recognize ligands in the apoptotic cell membrane that mimic oxLDL structure (11). Consistent with this, the present studies demonstrated partial competition of apoptotic cell phagocytosis by macrophages in the presence of excess oxPC-containing SUVs. Although many receptors have been implicated, similar to oxLDL recognition, little is known

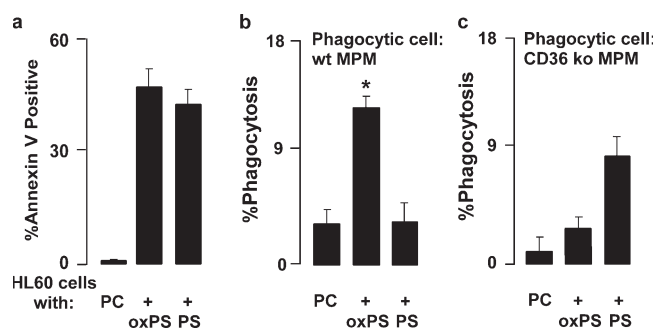


Figure 7. WT MPMs phagocytose viable (nonapoptotic) HL60 cells enriched with oxPS but not PS. 10^6 HL60 cells/ml were enriched with 2 mg of lipid vesicles in 1 ml PBS (either POPC carrier alone or carrier + 16 mol% of either PAPS or oxidized PAPS) for 30 min at 37°C, as described in Materials and methods. Cells were washed and stained with annexin V or overlaid onto MPMs. (a) Nonapoptotic cells were stained with FITC-labeled annexin V. Note that the addition of external carrier POPC failed to promote annexin V staining, whereas external incorporation of either PS or oxPS within carrier POPC similarly enhanced annexin V staining of cells. (b and c) Nonapoptotic cells labeled with external POPC carrier alone, or POPC + either PS or oxPS, and used in phagocytosis assay were overlaid onto either CD36 WT (b) or CD36-null (c) MPMs. *, $P < 0.02$ versus control.

regarding the precise nature of the ligands on apoptotic cell membranes that are recognized by phagocytes.

Although PS has traditionally been referred to as the “eat-me” signal for receptor-mediated phagocytosis of apoptotic cells, a role for PS oxidation in generating this signal has been less clear. The present studies strongly argue that virtually all of CD36-mediated PS recognition is via oxPS species. Indeed, PS commonly used in the literature likely contains substantial amounts of oxPS, particularly when methodologies used to prepare PS liposomes induce oxidation, such as sonication and dialysis in the absence of both antioxidants and chelating agents for redox active transition metals (8, 9, 25, 29). Moreover, sources of PS used in published studies are typically derived from brain or liver and contain large amounts of polyunsaturated fatty acid species susceptible to oxidation. Mass spectrometry analyses of multiple commercial sources of PS all showed readily measurable levels of oxPS_{CD36} (unpublished data). Further, in liposome binding studies with incorporation of low molar percent (10 mol%) PS derived from brain (without any prior HPLC reisolation to remove contaminant oxPS species), considerable binding to CD36 is readily observed in a dose-dependent manner. In contrast, incorporation of comparable levels of less oxidizable PS species (e.g., POPS or 1,2-dipalmitoyl-*sn*-glycero-3-phosphoserine) shows nominal background binding levels. It is thus our belief that oxPS may have accounted for observed CD36 binding activity in many previously published studies (8, 9, 25, 26, 29) demonstrating a role for CD36–PS interactions during phagocytosis of apoptotic cells.

A growing body of evidence indicates the involvement of oxidized phospholipids as pattern recognition ligands for

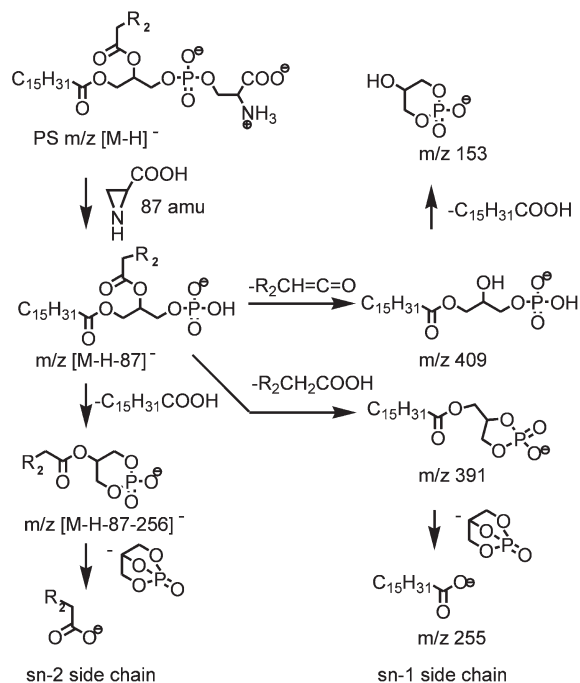


Figure 8. Common fragmentation pattern of PS molecular species during negative ion chemical ionization electrospray ionization mass spectrometry. Shown are common fragmentation pathways for PS molecular species under negative ion electrospray ionization mass spectrometry conditions. The origins of multiple common and specific ions for PS molecular species are illustrated. The neutral loss corresponding to the aziridine-2-carboxylic acid daughter accounts for the characteristic loss of 87.0 amu.

scavenger receptors on phagocytic cells. Our current data strongly support this hypothesis, focusing attention on CD36 and the sn-2 acyl moiety of oxPS, and to a lesser extent oxPC, as critical for apoptotic cell recognition. It is interesting to note that Kagan et al. have suggested the importance of oxidized PS ligands in apoptotic cell membranes required for efficient phagocytosis and clearance by mouse macrophages (27). However, neither the specific receptors involved nor the candidate ligands were identified. The range and complexity of the full spectra of oxPS species suggests that multiple potential ligands may be generated. Several oxPS species detected share the identical sn-2 oxidized fatty acids as observed in oxPC_{CD36} analogues (23, 24). That the indicated oxPS species (Table I and Fig. 9) are present in apoptotic membranes is strongly supported, however, by the extensive characterization of the fragmentation pattern of MS2 and MS3 daughter ions, as well as comparison with the known fragmentation pattern of the oxidized sn-2 fatty acids in synthetic oxPC species. The MSⁿ data thus provide strong corroboration that the phosphoserine headgroup-containing structural analogues of the oxPC_{CD36} ligands are indeed formed during apoptosis.

Our phagocytosis competition assay and PS lipid membrane enrichment assay both indicate that CD36 is the predominant

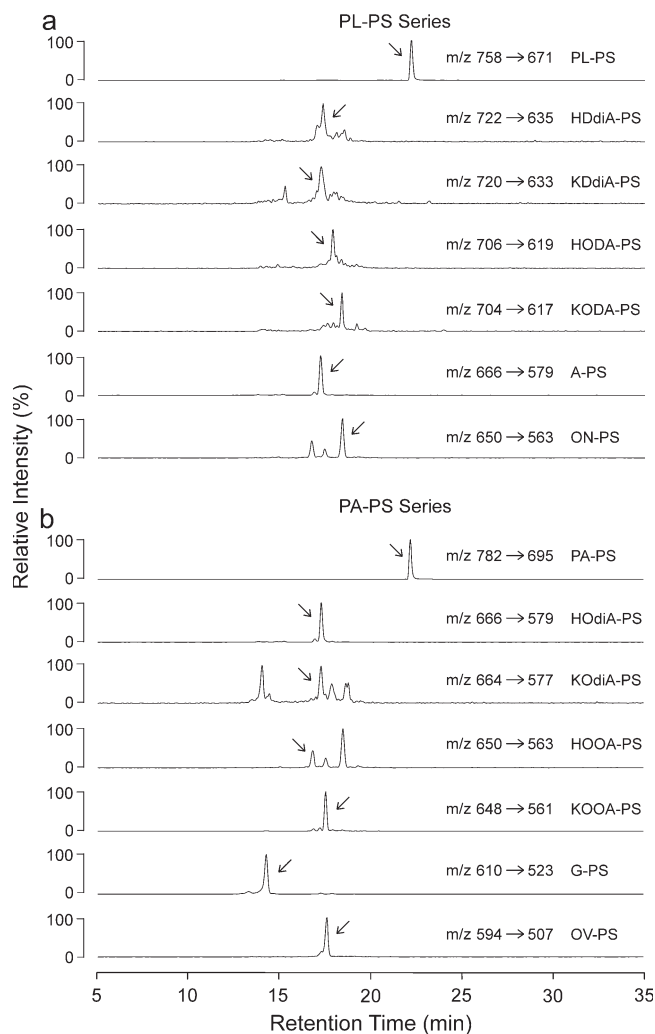


Figure 9. Demonstration of oxidized PS species in apoptotic membranes using negative ion LC/MS/MS. The presence of oxidized PAPS or PLPS species in lipid extracts of apoptotic cells was analyzed by HPLC with on-line negative ion electrospray ionization tandem mass spectrometry. Separation was done on a reverse phase C18 column (2.1 × 250 mm, 5 μm) using methanol/water as mobile phase at a flow rate of 0.2 ml/min with gradient and oxidized PLPS (a) and PAPS (b) molecular species identified by their characteristic retention time and daughter ions specific for each analyte, as described in Materials and methods.

receptor for oxPS on the surface of CD36 WT macrophages. Intriguingly, CD36-null macrophages phagocytose both PS liposomes and viable HL60 cells enriched with PS at the plasma membrane more efficiently than oxPS liposomes or oxPS-enriched cells. We can speculate that in the absence of the CD36 receptor, alternate receptors may be overexpressed as a compensatory adaptation and that these receptors bind PS with a higher affinity. We have examined the expression levels of SRA and PSR in WT and CD36 KO MPMs by both immunostaining and Western blot analyses and see no important differences at the protein level, suggesting that SRA and PSR are not the up-regulated receptor in the CD36 KO

MPMs (unpublished data). Although a consensus on the molecular identity and characteristics of a macrophage PSR has been questioned by some (30, 31), we at present do not know the identity of the PS binding receptor that is up-regulated in the CD36 KO MPMs.

It is intriguing to consider that, similar to uptake of oxLDL, recognition of common oxidation motifs by multiple phagocyte cell surface receptors has been exploited in such an evolutionarily conserved cellular process as apoptotic cell recognition and removal. Further understanding and characterization of scavenger receptor-oxidized phospholipid ligand interactions and downstream cellular consequences triggered by engagement of structurally specific oxPC and oxPS ligands is of interest.

MATERIALS AND METHODS

Materials. Unless otherwise indicated, lipids were purchased from Avanti Polar Lipids, Inc. and were confirmed to be >98% pure by mass spectrometry analyses. In an effort to remove trace levels of oxPS species present in even the best commercial PS sources, the oxidant-sensitive PS species PLPS and PAPS were purified by preparative HPLC and stored under argon atmosphere within amber vials at -80°C . CellTracker Green 5-chloromethylfluorescein diacetate (CMFDA; Invitrogen) and Di-I were obtained from Invitrogen. All other reagents were purchased from either Sigma-Aldrich or Fisher Scientific, unless otherwise specified. Anti-mouse CD36 antibody was made as described previously (32), anti-Fas clone CH-11 was obtained from Upstate Biotechnology, and anti-human CD36-phycoerythrin, anti-phosphatidyl serine receptor (human), and annexin V-FITC apoptosis detection kits were from BD Biosciences.

Cell Culture. Human chronic myelogenous leukemia cells (K562), promyelocytic leukemia cells (HL60), human Jurkat T cells, and primary MPMs were cultured in RPMI 1640 supplemented with 10% fetal bovine serum and penicillin/streptomycin antibiotics. African green monkey kidney fibroblasts (Cos-7) were cultured in DMEM supplemented with 10% fetal bovine serum and pen/strep antibiotics.

Construction of plasmids and transfections. Open reading frame encoding WT CD36 protein was subcloned into pCGCG (33) bicistronic expression vector containing GFP under translational control of a picornavirus (EMCV) IRES. This plasmid is referred to as CD36,GFP (bicistronic) in Fig. 2. Cells were transfected with 20 μg DNA in media made to 150 mM NaCl supplemented with 10 mM Hepes, pH 7.4, using an electroporator (Gene Pulser; Bio-Rad Laboratories) at 950 μF and 230 (K562) or 200 (Cos-7) V. Time constants were typically in the range of 44–48 ms.

Vesicle preparation and modification. 2-mg/ml stock solutions of SUVs comprised of PLPS, PAPS, POPS, or POPC with varying mole percents of specific oxidized phospholipids were prepared in argon-sparged sodium phosphate buffer by extrusion (11 times) through a 0.1-μm polycarbonate filter using a Mini-Extruder set (Avanti Polar Lipids) at 37°C . For a typical experiment, the relatively nonoxidizable phospholipid POPC was used as carrier, and the specified PS species was incorporated as a minor component (20 mol% or less, as indicated in the figures). For direct binding experiments, 1 mol% of Di-I was dried down together with the phospholipids indicated in the figures and incorporated into lipid vesicles by extrusion. CD36 ligands were isolated from PAPS or PLPS vesicles after oxidation by exposure to 30 mM MPO, an H_2O_2 -generating system comprised of 100 μM glucose and 100 ng/ml glucose oxidase, and 0.5 mM NaNO_2 at 37°C for 18 h. Reactions were stopped by the addition of 40 μM butylated hydroxytoluene and 300 nM catalase and stored under argon atmosphere at -80°C until use in cell binding studies. oxLDL was used as a prototypic ligand for CD36. It was formed as described by exposure of

isolated human LDL to the MPO-H₂O₂-NO₂⁻ system (34). Previous experiments have demonstrated that CD36 is the major receptor on MPMs that recognize LDL oxidized by this physiological method (17).

Flow cytometry and fluorescent microscopy analysis. Flow cytometry studies were performed on a FACScan (Becton Dickinson). For binding studies, 2×10^5 cells in 200 μ l (as indicated in the figures) were incubated with 500 μ g/ml Di-I-labeled liposomes at 4°C for 30 min to 1 h. Although cells incubated with Di-I-labeled liposomes at 37°C for 2 h (binding and uptake) showed similar results, we only present the binding (4°C) data. After incubation, cells were pelleted, washed three times with PBS containing 0.1% BSA, and resuspended in 400 μ l for immediate analysis. For fluorescent microscopy, cells were grown on glass coverslips and incubated with Di-I-labeled oxLDL or liposomes at 4°C for 30 min. After incubation, cells were fixed with 3.7% paraformaldehyde for 20 min and mounted on glass slides with VectaShield mounting media (Vector Laboratories). Fluorescent microscopy studies were performed on a microscope (DMR; Leica) and CCD camera (EX1; QImaging), and images were processed on Image-Pro software.

Phagocytosis assays. Suspension cells were rendered apoptotic after 254 nm UV irradiation for either 5 min (HL60) or 10 min (Jurkat). The cells were then cultured an additional 2–3 h before use. Apoptosis was also induced in Jurkat cells by incubating for 6 h at 37°C with 20 ng/ml anti-Fas antibody. Apoptosis was confirmed by multiple independent methods, including annexin V-FITC staining (>50% annexin V positive), DNA laddering assay, and nuclear morphology. 10^6 apoptotic cells were then layered over a monolayer (10^5) of adherent cells (CD36- or vector-transfected Cos-7 cells or MPMs) cultured on glass coverslips and co-cultured in 200 μ l DMEM (Cos-7) or RPMI 1640 (MPM) media for 1 h at 37°C. After incubation, unbound apoptotic cells were removed by extensive washing with media and then with PBS. Bound or ingested HL60 cells were visualized by *in situ* peroxidase staining (for HL60 MPO) with dimethylbenzidine, a peroxidase substrate (35). In brief, cells were incubated in 200 μ l 0.1 M NaPO₄, pH 6.2, followed by addition of 20 μ l 0.05% H₂O₂ and 20 μ l 1.25 mg/ml dimethoxybenzidine. Color development was stopped after 15–30 min by washing the coverslip with PBS and mounting in Vectashield mounting media on a glass slide. Bound or ingested Jurkat cells were detected by their green fluorescence after labeling with CellTracker Green CMFDA (according to manufacturer's instructions) before UV irradiation. Ingested cells were counted using Image-Pro software in at least four microscopic fields (300 cells/field). The bound and ingested apoptotic cells (HL60 or Jurkat) and the adherent cells (Cos-7 or MPM) were counted using Image-Pro software, and the percent phagocytosis was calculated by dividing the number of apoptotic cells ingested or bound by the total number of adherent phagocytizing cells in the monolayer (Cos-7 or MPM). For PS and oxPS competition experiments, 100 μ l PS or oxPS vesicles (2 mg/ml) were mixed with 100 μ l of control or apoptotic HL60 cells (10^6) and overlaid onto phagocytic cells (MPM or Cos-7) for 1 h at 37°C. Subsequent processing and analysis of bound and ingested cells was done as described.

MPMs. CD36 KO mice backcrossed >6 generations on a C57BL/6 background, along with C57BL/6 parent colonies, were used for these studies. Mice were injected intraperitoneally with 1 ml thioglycollate media (4% in H₂O), and cells were harvested by peritoneal lavage with sterile PBS/RPMI 1640 (1:1) at 4 d after injection to maximize CD36 surface expression. Approximately 10^5 cells were plated on sterile glass coverslips in complete RPMI 1640 media. All animal studies were performed using approved protocols from the Animal Research Committee of the Cleveland Clinic Foundation.

PS and oxPS enrichment of HL60 cell membranes. Cell membranes were enriched with PS or oxPS species by co-incubation of liposomes with cells using an adaptation of the methods described by Fadok et al. (29). In brief, lipid vesicles were extruded in 1 ml PBS at 2 mg/ml under inert

(argon) atmosphere. 10^6 HL60 cells were pelleted and resuspended in a 1-ml suspension of 2 mg/ml lipid of the lipid vesicles indicated in the figures and incubated for 30 min at 37°C. After incubation, cells were washed two times with PBS and stained with annexin V and propidium iodide according to manufacturer's instructions (annexin V-FITC apoptosis detection kit; BD Biosciences), or overlaid onto 10^5 MPMs cultured on glass coverslips and further incubated in RPMI 1640 media for an additional 2 h, and used in the phagocytosis assay.

Wound analysis. 2-mo-old background- and gender-matched WT (C57BLK6) and CD36 KO (backcrossed more than six generations) mice were anesthetized, and 6-mm punch biopsies were created on the lower left or right quadrant of the shaved dorsum. The wounds were left uncovered and monitored daily, and at the indicated timed points excised, fixed in 10% formalin, paraffin embedded, and sectioned at an 8- μ m thickness. Apoptotic cells in paraffin-embedded sections were identified using a fluorescein DNA fragmentation detection kit (QIA39; Calbiochem). For each wound section, the number of fluorescent cells was counted in three to five random low-power fields (20 \times).

Statistics. The results are presented as mean \pm SE values from at least three independent experiments, and statistical analyses were performed by the paired Student's *t* test.

Mass spectrometry. Lipids were initially extracted three times by the method of Bligh and Dyer (36). The combined extracts were rapidly dried under nitrogen and stored under an argon atmosphere at -80°C until analysis within 24 h. Mass spectra were acquired in negative ion mode using an LCQ ion trap mass spectrometer (LCQ; Thermo Finnigan) coupled with an electrospray ionization source. Capillary temperature was set at 300°C, and spray voltage was set at 4 kV. The fluid was nebulized using nitrogen as the sheath gas flow at 10 au, the auxiliary gas flow at 5 au, and the sweeping gas flow at 5 au. All data were collected using the data-dependent MSⁿ function. Full spectra were collected from *m/z* 100 to 1,200. Collision-induced dissociation was performed in the collision cell using He as the collision gas. All data were analyzed with Finnigan Xcalibur 1.4. The sample was dissolved in a mixture of methanol and chloroform (4:1, vol/vol), and both were infused directly into the mass spectrometer through a syringe pump at 3 μ l/min, as well as via HPLC interface after reverse phase separation. MSⁿ data of each compound are tabulated in Table I. Oxidized PS mixtures were characterized after reverse phase HPLC both on the LCQ ion trap instrument as described and on a triple quadrupole mass spectrometer (Quattro Ultima; Micromass). Each sample preparation (in 90% methanol) was injected onto a reverse phase C18 HPLC column (2 \times 150 mm, 5 μ m; ODS; Phenomenex) at a flow rate of 0.2 ml/min. oxPSes were resolved using a gradient from water containing 0.2% ammonium to methanol containing 0.2% ammonium. The column was equilibrated with 50% methanol and held at this composition for 6 min after the injection. A linear gradient was then run from 50 to 100% methanol over 10 min. The solvent composition was held at 100% methanol for 13 min. For analyses on the Quattro Ultima, the mass spectrometer was configured with the capillary voltage at 3 kV, the cone voltage at 40 V, the source temperature at 120°C, and a desolvation temperature at 250°C. The flow rate for the nitrogen in the cone and desolvation gas was 100 and 800 L/h, respectively. Collision-induced dissociation was obtained using argon gas. Analyses were performed using electrospray ionization in the negative-ion mode with multiple reaction monitoring of parent [M-H] and characteristic daughter ions [M-H-87]. The *m/z* of the individual transitions monitored is shown in Fig. 9. Because of the resolution of the mass spectrometer and the complexity of the sample, multiple interfering peaks were also detected in some traces. To distinguish the peaks of target compounds from the interfering peaks, online MS/MS spectra of expected *m/z* of postulated compounds were collected (unpublished data) and compared with the spectra obtained by LCQ. The peaks that failed to display characteristic sn-2 side chain ions in the MS/MS spectra were identified as interference. Fragmentation patterns of native and oxPS species were confirmed to follow common pathways as previously reported by Pulfer and Murphy (28).

We thank Quan Liu for contributions to the wound healing studies, Cathy Shemo and Sage O'Bryant for expert help with flow cytometry, and Amit Vasani for expert help with microscopy.

This work was supported by the National Institutes of Health (grants P01 HL076491, P01 HL77107, HL70621, and HL61878) and the Cleveland Clinic Foundation General Clinical Research Center (grant M01 RR018390).

The authors have no conflicting financial interests.

Submitted: 15 February 2006

Accepted: 5 October 2006

REFERENCES

- Henson, P.M., D.L. Bratton, and V.A. Fadok. 2001. Apoptotic cell removal. *Curr. Biol.* 11:R795–R805.
- Savill, J., and V. Fadok. 2000. Corpse clearance defines the meaning of cell death. *Nature.* 407:784–788.
- Meagher, L.C., J.S. Savill, A. Baker, R.W. Fuller, and C. Haslett. 1992. Phagocytosis of apoptotic neutrophils does not induce macrophage release of thromboxane B2. *J. Leukoc. Biol.* 52:269–273.
- Gao, Y., J.M. Herndon, H. Zhang, T.S. Griffith, and T.A. Ferguson. 1998. Antiinflammatory effects of CD95 ligand (FasL)–induced apoptosis. *J. Exp. Med.* 188:887–896.
- Endemann, G., L.W. Stanton, K.S. Madden, C.M. Bryant, R.T. White, and A.A. Protter. 1993. CD36 is a receptor for oxidized low density lipoprotein. *J. Biol. Chem.* 268:11811–11816.
- Rigotti, A., S.L. Acton, and M. Krieger. 1995. The class B scavenger receptors SR-BI and CD36 are receptors for anionic phospholipids. *J. Biol. Chem.* 270:16221–16224.
- Daviet, L., and J.L. McGregor. 1997. Vascular biology of CD36: roles of this new adhesion molecule family in different disease states. *Thromb. Haemost.* 78:65–69.
- Fadok, V.A., M.L. Warner, D.L. Bratton, and P.M. Henson. 1998. CD36 is required for phagocytosis of apoptotic cells by human macrophages that use either a phosphatidylserine receptor or the vitronectin receptor (alpha v beta 3). *J. Immunol.* 161:6250–6257.
- Tait, J.F., and C. Smith. 1999. Phosphatidylserine receptors: role of CD36 in binding of anionic phospholipid vesicles to monocytic cells. *J. Biol. Chem.* 274:3048–3054.
- Febbraio, M., D.P. Hajjar, and R.L. Silverstein. 2001. CD36: a class B scavenger receptor involved in angiogenesis, atherosclerosis, inflammation, and lipid metabolism. *J. Clin. Invest.* 108:785–791.
- Savill, J., I. Dransfield, C. Gregory, and C. Haslett. 2002. A blast from the past: clearance of apoptotic cells regulates immune responses. *Nat. Rev. Immunol.* 2:965–975.
- Ren, Y., R.L. Silverstein, J. Allen, and J. Savill. 1995. CD36 gene transfer confers capacity for phagocytosis of cells undergoing apoptosis. *J. Exp. Med.* 181:1857–1862.
- Albert, M.L., S.F. Pearce, L.M. Francisco, B. Sauter, P. Roy, R.L. Silverstein, and N. Bhardwaj. 1998. Immature dendritic cells phagocytose apoptotic cells via $\alpha v \beta 5$ and CD36, and cross-present antigens to cytotoxic T lymphocytes. *J. Exp. Med.* 188:1359–1368.
- Coburn, C.T., T. Hajri, A. Ibrahim, and N.A. Abumrad. 2001. Role of CD36 in membrane transport and utilization of long-chain fatty acids by different tissues. *J. Mol. Neurosci.* 16:117–121.
- Ibrahim, A., and N.A. Abumrad. 2002. Role of CD36 in membrane transport of long-chain fatty acids. *Curr. Opin. Clin. Nutr. Metab. Care.* 5:139–145.
- Jimenez, B., O.V. Volpert, S.E. Crawford, M. Febbraio, R.L. Silverstein, and N. Bouck. 2000. Signals leading to apoptosis-dependent inhibition of neovascularization by thrombospondin-1. *Nat. Med.* 6:41–48.
- Podrez, E.A., M. Febbraio, N. Sheibani, D. Schmitt, R.L. Silverstein, D.P. Hajjar, P.A. Cohen, W.A. Frazier, H.F. Hoff, and S.L. Hazen. 2000. Macrophage scavenger receptor CD36 is the major receptor for LDL modified by monocyte-generated reactive nitrogen species. *J. Clin. Invest.* 105:1095–1108.
- Navazo, M.D., L. Daviet, J. Savill, Y. Ren, L.L. Leung, and J.L. McGregor. 1996. Identification of a domain (155–183) on CD36 implicated in the phagocytosis of apoptotic neutrophils. *J. Biol. Chem.* 271:15381–15385.
- Puente Navazo, M.D., L. Daviet, E. Ninio, and J.L. McGregor. 1996. Identification on human CD36 of a domain (155–183) implicated in binding oxidized low-density lipoproteins (Ox-LDL). *Arterioscler. Thromb. Vasc. Biol.* 16:1033–1039.
- Pearce, S.F., P. Roy, A.C. Nicholson, D.P. Hajjar, M. Febbraio, and R.L. Silverstein. 1998. Recombinant glutathione S-transferase/CD36 fusion proteins define an oxidized low density lipoprotein-binding domain. *J. Biol. Chem.* 273:34875–34881.
- Febbraio, M., N.A. Abumrad, D.P. Hajjar, K. Sharma, W. Cheng, S.F. Pearce, and R.L. Silverstein. 1999. A null mutation in murine CD36 reveals an important role in fatty acid and lipoprotein metabolism. *J. Biol. Chem.* 274:19055–19062.
- Nicholson, A.C., J. Han, M. Febbraio, R.L. Silverstein, and D.P. Hajjar. 2001. Role of CD36, the macrophage class B scavenger receptor, in atherosclerosis. *Ann. N. Y. Acad. Sci.* 947:224–228.
- Podrez, E.A., E. Poliakov, Z. Shen, R. Zhang, Y. Deng, M. Sun, P.J. Finton, L. Shan, M. Febbraio, D.P. Hajjar, et al. 2002. A novel family of atherogenic oxidized phospholipids promotes macrophage foam cell formation via the scavenger receptor CD36 and is enriched in atherosclerotic lesions. *J. Biol. Chem.* 277:38517–38523.
- Podrez, E.A., E. Poliakov, Z. Shen, R. Zhang, Y. Deng, M. Sun, P.J. Finton, L. Shan, B. Gugu, P.L. Fox, et al. 2002. Identification of a novel family of oxidized phospholipids that serve as ligands for the macrophage scavenger receptor CD36. *J. Biol. Chem.* 277:38503–38516.
- Ryeom, S.W., R.L. Silverstein, A. Scotto, and J.R. Sparrow. 1996. Binding of anionic phospholipids to retinal pigment epithelium may be mediated by the scavenger receptor CD36. *J. Biol. Chem.* 271:20536–20539.
- Yamaguchi, A., N. Yamamoto, N. Akamatsu, T.C. Saido, M. Kaneda, M. Umeda, and K. Tanoue. 2000. PS-liposome and ox-LDL bind to different sites of the immunodominant domain (#155–183) of CD36: a study with GS95, a new anti-CD36 monoclonal antibody. *Thromb. Res.* 97:317–326.
- Kagan, V.E., B. Gleiss, Y.Y. Tyurina, V.A. Tyurin, C. Elenstrom-Magnusson, S.X. Liu, F.B. Serinkan, A. Arroyo, J. Chandra, S. Orrenius, and B. Fadeel. 2002. A role for oxidative stress in apoptosis: oxidation and externalization of phosphatidylserine is required for macrophage clearance of cells undergoing Fas-mediated apoptosis. *J. Immunol.* 169:487–499.
- Pulfer, M., and R.C. Murphy. 2003. Electrospray mass spectrometry of phospholipids. *Mass Spectrom. Rev.* 22:332–364.
- Fadok, V.A., A. de Cathelineau, D.L. Daleke, P.M. Henson, and D.L. Bratton. 2001. Loss of phospholipid asymmetry and surface exposure of phosphatidylserine is required for phagocytosis of apoptotic cells by macrophages and fibroblasts. *J. Biol. Chem.* 276:1071–1077.
- Bose, J., A.D. Gruber, L. Helming, S. Schiebe, I. Wegener, M. Hafner, M. Beales, F. Kontgen, and A. Lengeling. 2004. The phosphatidylserine receptor has essential functions during embryogenesis but not in apoptotic cell removal. *J. Biol.* 3:15.
- Williamson, P., and R.A. Schlegel. 2004. Hide and seek: the secret identity of the phosphatidylserine receptor. *J. Biol.* 3:14.
- Finnemann, S.C., and R.L. Silverstein. 2001. Differential roles of CD36 and $\alpha v \beta 5$ integrin in photoreceptor phagocytosis by the retinal pigment epithelium. *J. Exp. Med.* 194:1289–1298.
- Greenberg, M.E., A.J. Iafate, and J. Skowronski. 1998. The SH3 domain-binding surface and an acidic motif in HIV-1 Nef regulate trafficking of class I MHC complexes. *EMBO J.* 17:2777–2789.
- Podrez, E.A., D. Schmitt, H.F. Hoff, and S.L. Hazen. 1999. Myeloperoxidase-generated reactive nitrogen species convert LDL into an atherogenic form in vitro. *J. Clin. Invest.* 103:1547–1560.
- Henson, P.M., B. Zanolari, N.A. Schwartzman, and S.R. Hong. 1978. Intracellular control of human neutrophil secretion. I. C5a-induced stimulus-specific desensitization and the effects of cytochalasin B. *J. Immunol.* 121:851–855.35.
- Bligh, E.G., and W.J. Dyer. 1959. A rapid method of total lipid extraction and purification. *Can. J. Biochem. Physiol.* 37:911–917.